ARTICLE IN PRESS

Available online at www.sciencedirect.com

SCIENCE DIRECT®

ELSEVIER

Solar Energy xxx (2005) xxx–xxx

SOLAR ENERGY

www.elsevier.com/locate/solener

Solar chimney power plants for high latitudes

E. Bilgen *, J. Rheault

Departement de Genie Mecanique, Ecole Polytechnique, C.P. 6079, centre ville, Montreal, Que., Canada H3C 3A7

Received 15 July 2004; received in revised form 3 December 2004; accepted 10 January 2005

Communicated by: Associate Editor S.A. Sherif

Abstract

A solar chimney system for power production at high latitudes has been designed and its performance has been evaluated. A mathematical model and a code on MATLAB platform have been developed based on monthly average meteorological data and thermodynamic cycle. The thermal performance of a 5 MW nominal power production plant at three locations in Canada, namely Ottawa, Winnipeg and Edmonton, is studied. The sloped collector field is built at suitable mountain hills, which also functions as a chimney. Then a short vertical chimney is added to install the vertical axis air turbine. The results showed that solar chimney power plants at high latitudes may have satisfactory thermal performance and produce as much as 85% of the same plants in southern locations with horizontal collector field. The overall thermal performance of these plants is a little less than 0.5%.

Keywords: Solar chimney; Solar power; High latitude

1. Introduction

The solar chimney concept was proposed in 1970s by Schlaich and later in 1980s studies were carried out with a 50 kW power prototype in Manzanares, Spain (Haaf et al., 1983). The prototype had about 11 000 m^2 collector installed on a horizontal land area, 200 m high and 10 m diameter chimney, and a 50 kW nominal power turbine. The three important parts of a solar chimney power plant are the collector system, the chimney and the air turbine as shown in Fig. 1(a). Ambient air enters the collector system from the periphery of the collector and heated mainly by convection along the hot ground. It enters at the bottom of the chimney due to pressure potential generated by the difference of density between the warm air and ambient air. Some of the pressure potential is used by pressure losses due to friction through the collector and chimney, loss coefficients, drags in collector and chimney, kinetic energy changes in various parts of the system such as contractions and diffuser section, and a remaining part for flow through and pressure drop in the turbine. Using a thermodynamic analysis, it can easily be shown that the power generated by solar chimney system is directly proportional to chimney height, H_T, collector size D_{col}^2 and solar radiation, G. One important parameter in this relationship is the solar radiation received by the collector system. For this reason solar chimney power plants studied in the literature are conceived for low latitudes with horizontal collector systems, such as the Manzanares prototype or the planned 200 MW

* Corresponding author. Tel.: +1 514 340 4711x4579; fax +1 514 340 5917.

E-mail address: bilgen@polymtl.ca (E. Bilgen).

0038-092X/$ - see front matter © 2005 Published by Elsevier Ltd.
doi:10.1016/j.solener.2005.01.003

Nomenclature

A	area
c_p	heat capacity
G_{sc}	solar constant
$\bar{H}$	monthly average daily radiation on a horizontal surface
$\bar{H}_T$	monthly average daily total radiation on sloped surface
$\bar{H}_v$	monthly average daily beam radiation
$\bar{H}_d$	monthly average daily diffuse radiation
$\bar{H}_g$	monthly average daily ground radiation
$\bar{H}_0$	monthly average daily extraterrestrial radiation on horizontal surface
h_w	wind convection coefficient
$\bar{K}_T$	monthly average daily clearness index
$\dot{m}$	mass flow rate
n	average day of the month
N	number of glass cover
Nu	Nusselt number
$\bar{q}_u$	useful heat flux
$\bar{Q}_u$	useful heat
q_t	top losses
$\bar{R}_b$	monthly average beam radiation
Ra	Rayleigh number
$\bar{S}$	monthly average daily radiation absorbed by a sloped surface
T	temperature
U_L	overall loss coefficient
U_t	top loss coefficient
U_b	bottom loss coefficient
V_w	wind velocity

Greek symbols

α	absorption coefficient
$\bar{\alpha}$	monthly average ground absorption coefficient
β	slope
δ	declination
ϵ	emittance
η	efficiency
θ	incidence angle
ρ_g	albedo
σ	Stefan–Bolzmann constant
τ	transmission coefficient, time
$\bar{\tau}$	monthly average transmission coefficient
$\overline{(\tau\alpha)}$	monthly average transmittance–absorbance product
ϕ	latitude
ω_s	sunset hour angle

Subscripts

a	air, ambient
b	beam
c	cover
chi	chimney
col	collector
d	diffuse
f	friction
g	ground
KE	kinetic energy
o	ambient
p	plate, ground
r	reflection, radiation
t	turbine, transmitted
tot	total

solar chimney system to be built in Mildura, Australia within the next two years (Enviromission, 2004). The planned Mildura solar chimney plant will have 12.5 million m^2 collector area and 1000 m high chimney.

Yet there are many locations in northern latitudes from 45° to 55°, where sloped lands are readily available and sunshine is at acceptable levels. Designing solar chimney collector system on sloped surface or suitable hills has two major advantages: first, if the collector slope is optimized, the solar radiation received by the collector system may be improved to a satisfactory level for a year round operation and the second, a sloped surface constitutes a natural chimney, therefore the chimney height standing above the collector height may be reduced considerably, thus reducing civil engineering problems and cost.

The objectives of this study are:

- To develop a simplified solar chimney plant simulation method and a computer program.
- To verify the method and the program against available data in the literature.
- To carry out a thermal performance study for locations in northern latitudes.
- To do a sensitivity analysis to determine the relative importance of various parameters.

2. System description

The solar chimney power plant system studied consists of the following major components: sloped collec-

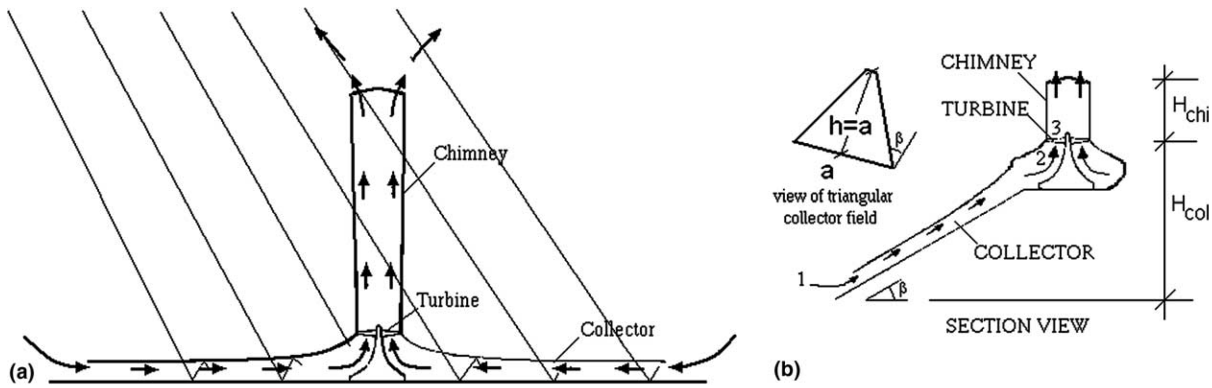

Fig. 1. Schematic of the solar chimney: (a) systems on horizontal surface at low latitudes, (b) systems in sloped surface at high latitudes.

tor, chimney and turbine as shown in Fig. 1(b). The collector has a triangular surface area with a chimney at its apex. The sides are closed, the air enters from the lower side and rises as heated by the ground to the apex where a short chimney is installed vertically.

3. Mathematical model and code

The simulation model and the code were developed following the methods for evaluating long term solar system performance using the monthly average absorbed radiation. The meteorological data required are monthly average solar radiation on a horizontal surface, monthly average air temperature and wind velocity for a typical day of each month.

The simulation code consists of the following:

- the mathematical model to calculate the solar radiation received by sloped collector;
- the optimization model to determine optimum slope based on annual maximum solar energy;
- the model to calculate the pressure drops due to friction, form drag and contractions;
- the thermodynamic model to calculate the total pressure and velocity generated in the chimney, and generated power.

These models are briefly reviewed in the following sections.

3.1. Solar radiation model

The solar energy received by a sloped surface is determined using the monthly average daily total radiation on a horizontal surface, $\bar{H}$. The algorithm to calculate the monthly average of daily total radiation on a tilted surface at a given location, for a particular day, follows the well established methods in the literature (e.g., Duffie and Beckman, 1991).

The monthly average extraterrestrial radiation on a surface is

$$\bar{H}_0 = \frac{24\,3600 G_{sc}}{\pi}\left(1 + 0.033\cos\frac{360n}{365}\right. \times \left.\left(\cos\phi\cos\delta\sin\omega_s + \frac{\pi\omega_s}{180}\sin\phi\sin\delta\right)\right) \quad (1)$$

where

$$\delta = 23.45\sin\left(360\frac{284+n}{365}\right) \quad (2)$$

$$\omega_s = a\cos(-\tan\phi\tan\delta) \quad (3)$$

The monthly average daily clearness index $\bar{K}_T$ is calculated as

$$\bar{K}_T = \frac{\bar{H}}{\bar{H}_0} \quad (4)$$

The diffuse component of the monthly average daily radiation is calculated as

For $0.3 < \bar{K}_T < 0.8$ and $\omega_s < 81.4°$:

$$\bar{H}_d = \bar{H}_T(1.311 - 3.022\bar{K}_T + 3.427\bar{K}_T^2 - 1.821\bar{K}_T^3) \quad (5)$$

For $0.3 < \bar{K}_T < 0.8$ and $\omega_s > 81.4°$:

$$\bar{H}_d = \bar{H}_T(1.391 - 3.560\bar{K}_T + 4.189\bar{K}_T^2 - 2.137\bar{K}_T^3) \quad (6)$$

The monthly average of $\bar{R}_b$ is

$$\bar{R}_b = \frac{\cos(\phi-\beta)\cos\delta\sin\omega_s' + \frac{\pi}{180}\omega_s'\sin(\phi-\beta)\sin\delta}{\cos\phi\cos\delta\sin\omega_s + \frac{\pi}{180}\omega_s\sin\phi\sin\delta} \quad (7)$$

with

$$\omega_s' = \min[\cos^{-1}(-\tan\phi\tan\delta), \cos^{-1}(-\tan(\phi-\beta)\tan\delta)] \quad (8)$$

Finally the monthly average solar radiation on a south facing sloped surface is calculated as

$$\bar{S} = (\bar{H}_\mathrm{T} - \bar{H}_\mathrm{d})\bar{R}_\mathrm{b}\overline{(\tau\alpha)}_\mathrm{b} + \bar{H}_\mathrm{d}\overline{(\tau\alpha)}_\mathrm{d}\frac{1+\cos\beta}{2} + \bar{H}\rho_\mathrm{g}\overline{(\tau\alpha)}_\mathrm{g}\frac{1-\cos\beta}{2} \quad (9)$$

where the monthly average transmittance–absorptance product is

$$\overline{(\tau\alpha)} = \frac{\bar{S}}{\bar{H}_\mathrm{T}} \quad (10)$$

The monthly average of incidence angles of direct, diffuse and ground reflected radiations are

$$\left.\begin{aligned} \bar{\theta}_\mathrm{b} &= a\cos(\sin\delta\sin\phi\cos\beta - \sin\delta\cos\phi\sin\beta\cos\gamma \\ &\quad + \cos\delta\cos\phi\cos\beta\cos\omega + \cos\delta\sin\phi\sin\beta\cos\gamma\cos\omega \\ &\quad + \cos\delta\sin\beta\sin\gamma\sin\omega) \\ \bar{\theta}_\mathrm{d} &= 59.7 - 0.1388\beta + 0.001497\beta^2 \\ \bar{\theta}_\mathrm{g} &= 90 - 0.5788\beta + 0.002693\beta^2 \end{aligned}\right\} \quad (11)$$

where, in view of lack of an analytical expression, the monthly average incidence angle is approximated at 2.5 h from the solar noon in the average day of the month. The possible error in calculating $\bar{\theta}_\mathrm{b}$ by the approximate method was checked by running the code at slopes β from 30 to 50 at two latitudes $\phi = 40°$ and 50° and comparing the results against those of graphical solutions in (Klein, 1979). It was found that during winter months the agreement was acceptable. During summer months, the approximation resulted in maximum 20% smaller values. Further checking its effect on $\bar{H}_\mathrm{T}$ showed that it was less than 0.5%.

3.2. Transmission through the collector

The solar energy received by the collector is transmitted through a transparent cover and absorbed by the ground, which is heated up. A major part of the absorbed energy is transferred to the ambient air entering through the open periphery and exiting through the chimney. A part is lost by a combination of heat transfer, through the cover and ground, which are indeed similarly evaluated as for a flat plate air solar collector, by calculating so-called upward and back losses. The principal relations are as follows.

The ground absorption coefficient as a function of incident angle and the transmittance–absorptance product are

$$\left.\begin{aligned} \bar{\alpha} &= \bar{\alpha}_n(1 + 2.0345\times10^{-3}\bar{\theta} - 1.990\times10^{-4}\bar{\theta}^2 \\ &\quad + 5.324\times10^{-6}\bar{\theta}^3 - 4.799\times10^{-8}\bar{\theta}^4) \\ \overline{(\tau\alpha)} &= 1.01\times\bar{\tau}\bar{\alpha} \end{aligned}\right\} \quad (12)$$

where $\bar{\theta}$ takes the values for direct, diffuse and ground reflected incidence angles to calculate corresponding absorption coefficients, $\bar{\alpha}$.

The upward and ground losses are calculated following the well established relations and algorithm, and the overall loss coefficient $U_\mathrm{L} = U_\mathrm{t} + U_\mathrm{b}$ is calculated (see Fig. 2).

Top loss coefficient is calculated (e.g., Duffie and Beckman, 1991) as

$$\left.\begin{aligned} U_\mathrm{t} &= \frac{q_\mathrm{t}}{T_\mathrm{p} - T_\mathrm{a}} \\ q_\mathrm{t} &= \frac{T_\mathrm{p} - T_\mathrm{a}}{Nc^{-1}\left(\frac{T_\mathrm{p}-T_\mathrm{a}}{N+ff}\right)^{-0.25} + h_\mathrm{w}^{-1}} + \frac{\sigma(T_\mathrm{p}^4 - T_\mathrm{a}^4)}{\epsilon_\mathrm{p}^{-1} + \frac{2N+ff-1}{\epsilon_\mathrm{p}} - N} \\ c &= 1.2529 - 0.00651\beta + 0.0000267\beta^2 \\ ff &= 0.76 - 0.118V_\mathrm{w} + 0.0066V_\mathrm{w}^2 \\ h_\mathrm{w} &= 2.8 + 3.0V_\mathrm{w} \end{aligned}\right\} \quad (13)$$

Ground loss coefficient is calculated from (Ingersoll et al., 1954) as

$$U_\mathrm{b} = 2\left(\frac{k\rho c_\mathrm{p}}{\pi\tau}\right)^{0.5} \quad (14)$$

where the period $\tau = 86400$ s. We note that since the thermal simulation in this study is based on monthly average daily parameters, U_b is an average heat transfer coefficient estimated on the time constant surface temperature. The simulation of periodic and unsteady state case for heat storage and recuperation due to periodic heat transfer to and from the ground is beyond the capability of a monthly average daily simulation model. This aspect has been discussed by Haaf (1984), Haaf et al. (1983) and Bernardes et al. (2003). They show that heat storage, recuperation and running the system after sun set may be an advantageous aspect of the solar chimney systems if a proper design is implemented.

Convection coefficients, h_1 and h_2, are difficult to determine due to lack of suitable correlations for in-

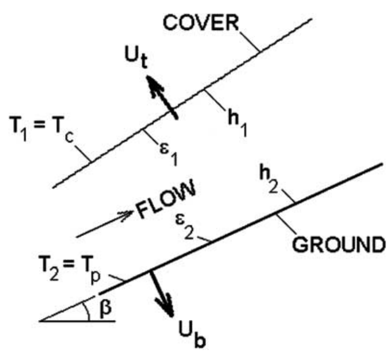

Fig. 2. Schematic of the collector system with relevant parameters used in the text.

clined plates and channels. In models published in the literature for solar chimney collector systems, the cover and ground are considered as horizontal plates (e.g. Pasumarthi and Sherif, 1998; Bernardes et al., 2003) and appropriate correlations are used. Strictly speaking the cover is not horizontal but sloped, but since the collector is analyzed as segments in the radial direction, it is a justified approximation. In our case, we use the same technique and assume the similar simplification of parallel plate geometry in each collector segment. Thus the correlation by Churchill and Chu (1975) for vertical plates using a modified Rayleigh number, $Ra\cos\beta$ can be used to estimate h_1 on the heated bottom surface of the inclined cover. For the top surface of the heated ground, a similar approximation is not recommended due to instabilities but other empirical relations (Fujii and Imura, 1972; Azevedo and Sparrow, 1985). If we assume the collector system is more like an open-ended channel, the empirical relation obtained for both sides heated inclined channels by Azevedo and Sparrow (1985) may also be used.

$$Nu = 0.645((S/L)Ra_S)^{1/4} \quad 0<\beta<45 \quad (S/L)Ra_S > 2\times10^2 \tag{15}$$

where S is the channel spacing, L is the channel length, $Ra_S = g\beta(T - T_i)S^3/\alpha\nu$ with surface temperature T, $\beta = 1/T_{fm}$ and the fluid properties evaluated at average fluid temperature, T_{fm}. It is a correlation combining the heat transfer results for various heating modes, inclinations, interplate spacings and modified Rayleigh numbers $(S/L)Ra_S$, i.e., insensitive to inclination and heating mode. In fact, we tested for the condition of this study the correlations of Churchill and Chu (1975), McAdams (1954), Fujii and Imura (1972), which are used by Pasumarthi and Sherif (1998) and Bernardes et al., 2003, and Eq. (15). We found that the differences in Nusselt numbers were small, which had a negligible effect on the simulation end results.

The radiation heat transfer coefficient between two parallel plates is

$$h_r = \frac{\sigma(T_2^2 + T_1^2)(T_2 + T_1)}{\epsilon_2^{-1} + \epsilon_1^{-1} - 1} \tag{16}$$

The collector efficiency, flow and heat removal factors are respectively

$$\left.\begin{aligned} F' &= \frac{h_r h_2 + h_2 U_t + h_1 h_r + h_2 h_1}{((U_t + h_r) + h_1)(U_b + h_2 + h_r) - h_r^2} \\ F'' &= \frac{\dot{m}c_p}{A_c U_L F'}\left(1 - \exp\left(\frac{-A_c U_L F'}{\dot{m}c_p}\right)\right) \\ F_R &= F'F'' \end{aligned}\right\} \tag{17}$$

The useful heat collected, Q_u or useful heat flux, q_u and the thermal collector efficiency, η_{col} are

$$\left.\begin{aligned} \bar{Q}_u &= A_c F_R(\bar{S} - U_L(T_i - T_a)) \\ \bar{q}_u &= F_R(\bar{S} - U_L(T_i - T_a)) \\ \eta_{col} &= \bar{q}_u/\bar{H}_T \end{aligned}\right\} \tag{18}$$

3.3. Chimney

Pressure developed due to air density difference between entrance at T_2 and exit at $T_0 \approx T_1$ in a chimney is calculated as

$$\Delta P = \int_1^2 g(\rho_0 - \rho(z))\,dz \tag{19}$$

For a vertical adiabatic chimney, by integrating Eq. (19) between entrance at temperature T_2 and exit at T_0, we obtain

$$\Delta P_{chi} = (\rho_0 - \rho_2)gH_{chi} \tag{20}$$

We assume that the air density variation is linear between entrance and exit of the sloped collector. Indeed, this hypothesis is justified because ΔT between air temperature at the entrance and exit of the collector is small, about 10–15 K and the radius of the collector field or the collector length in our case in combination with the chimney height is determined in such a way that solar heat is collected along the radial direction to have thermal parameters quasi-linear (Haaf et al., 1983; Bernardes et al., 2003). This is achieved by hourly simulation. Thus, the air density variation can be expressed as

$$\rho(z) = \rho_0 + \frac{\rho_2 - \rho_0}{H_{col}}z \tag{21}$$

By integrating Eq. (19) between entrance and exit of the sloped collector with $\rho(z)$ from Eq. (21), we obtain the pressure difference created in the collector

$$\Delta P_{col} = \frac{\rho_0 - \rho_2}{2}gH_{col} \tag{22}$$

As noted earlier, $T_0 \approx T_1$ hence the total pressure due to buoyancy is

$$\Delta P_{tot} = (\rho_1 - \rho_2)g\left(H_{chi} + \frac{H_{col}}{2}\right) \tag{23}$$

The total pressure difference so created is spent, in part, for friction losses in the collector and the chimney, ΔP_f, also kinetic energy losses at the chimney exit, ΔP_{KE}, and the rest is used by the turbine, ΔP_t. Thus,

$$\Delta P_{tot} = \Delta P_t + \Delta P_f + \Delta P_{KE} \tag{24}$$

with

$$\Delta P_f = f\frac{L}{D}\frac{1}{2}\rho V^2 \tag{25}$$

where f is the friction factor calculated by the Colebrook correlation, L, D and V take the length, equivalent diameter and velocity for the collector and chimney, and

$$\Delta P_{\mathrm{KE}} = \frac{1}{2}\rho V_{\mathrm{chi}}^2 \tag{26}$$

We note that the collector cover height from the ground is variable. The height is determined to have approximately the same cross section throughout as that of chimney.

3.4. Power and overall thermal efficiency

The power generated by the turbine, P_{t} and the overall thermal efficiency, η are respectively

$$P_{\mathrm{t}} = \eta_{\mathrm{t}}\Delta P_{\mathrm{t}} V_{\mathrm{chi}} A_{\mathrm{chi}} \tag{27}$$

$$\eta = CP_{\mathrm{t}}/\bar{H}_{\mathrm{T}} \tag{28}$$

where C = (s/day) is the power production duration in a given monthly average day.

3.5. Algorithm

The algorithm assumes that for a short collector, of order of magnitude of 10 m or less, the surrounding temperatures are uniform and the temperature of the air stream in the collector varies linearly along the collector, as discussed earlier. Thus, the collector is divided in short equal segments of collectors, and the parameters determined by computations in a previous segment are used as those at the entrance of the following segment. This technique is also used by Pasumarthi and Sherif (1998) and Bernardes et al. (2003). The iterative process is summarized below.

- Read geographic location (latitude, longitude, altitude), collector data (slope, number of covers, dimensions), cover material properties, ground optical characteristics. Read meteorological data (monthly average daily radiation on horizontal surface, temperature and wind velocity).
- Calculate monthly average incidence angles for diffuse and reflected radiations, and monthly average coefficients of reflection, transmission, absorption for these incidence angles.
- Calculate monthly average sun's position at noon and sunset hour angle, and incidence angle of direct beam radiation. Calculate monthly average coefficients of reflection, transmission, absorption for beam radiation.
- Calculate monthly average extraterrestrial radiation, clearness index, and monthly average total radiation on the collector.
- For a known air inlet temperature, input initial values for cover temperature, T_{c}, fluid temperature, T_{f}, average fluid temperature, T_{fm}, absorber temperature, T_{p}.
- Input initial value for air mass flow rate, $\dot{m}$.
- Iteration loop (to determine by iteration $\dot{m}$, T_{f}, T_{c} and T_{p}).
- Calculate convection heat transfer coefficients of wind, in the collector, and overall coefficient, U_{t}, U_{b}, U_{L}.
- Calculate F', F'', F_{R} and useful energy, $\bar{Q}_u$.
- Calculate $\dot{m}$ using the air velocity in the chimney (or using $\bar{Q}_u$).
- Calculate T_{f}, T_{fm} and T_{p} during which make use of two relations, one based on $\bar{Q}_u$ and the other on T_{fm} and T_i to calculate T_{f}.
- Check if $|T_{\mathrm{f}}(i) - T_{\mathrm{f}}(i-1)| < 0.1$; if not repeat the calculation starting at the iteration loop.
- Calculate power and monthly produced energy and other parameters.

3.6. Code and validation

A computer program was written on MATLAB platform and to make sure that the algorithm of radiation and transmission calculations produced correct results, the code was validated using various examples in the literature (e.g., Duffie and Beckman, 1991) in every step of the calculations of important parameters such as $\bar{H}_{\mathrm{T}}$, $\bar{S}$ and $\bar{Q}_{\mathrm{u}}$. The agreement was obtained within 2–3% for slopes from zero to 90°. A validation using a solar chimney power plant was however difficult due to lack of monthly average daily data in the literature. Nevertheless an attempt was made using the published results of the Manzanares prototype, which had a horizontal collector field, a chimney and a turbine (Haaf, 1984). Using September 2, 1982 data and his Fig. 12, we determined $\bar{H} \approx 22.8$ MJ/m^2/day and operation hour 9.6 h. The power varied from about 10–36 kW through the day, the average of which was determined at about 27 kW. In addition, the calculated power from the measured increase in air temperature varied from 10 to 50 kW, its daily average was determined at about 38.7 kW. The code was run to simulate the Manzanares plant using its parameters and data. It produced for September 15 the daily average power of 36 kW, which is higher by 33% from the average net power, and it is lower by about 5% from the calculated average power using the measured increase in air temperature.

4. Results and discussion

The study was carried out for three Canadian locations, Ottawa, Winnipeg and Edmonton for which monthly average meteorological data (solar radiation, temperature and wind velocity) are available. The locations were selected to obtain a wide range of latitudes, which varied from 45.5° to 53.6° north where the annual total radiation on horizontal surface, $\bar{H}$ are from 4.778 to 4.914 GJ/m^2/year.

Collector system oriented due south in northern hemisphere, the optimum slope for each location was first determined by a parametric analysis, the results of which are presented in Table 1. We also calculated for the optimum slope, the annual average solar radiation on the collector surface, $\Sigma\bar{H}_T$ in kW h/m^2/year for each location and presented in Table 1. We can see that to maximize solar radiation received by the collector system, the collector slope should be 5–7° smaller than the latitude, which is an expected result. The annual total solar radiation on horizontal surface is from 1299 to 1365 kW h/m^2/year for the same locations respectively. Theoretical annual operation time was calculated to be a little less than 3000 h for all three locations. We note that from the solar radiation point of view Winnipeg location seems to be the best among the three locations considered. These values may be compared to those reported for southern locations used in (Schlaich, 1995): $\Sigma\bar{H} = 2300$ kW h/m^2/year and annual full load hours = 2780–3052 h.

Solar chimney system: we selected the solar chimney power plant of 5 MW nominal power reported by Schlaich (1995) and carried out a thermodynamic study to determine the preliminary design parameters and base dimensions for simulation. The constant parameters for the all cases were identical, except the collector and chimney heights, for which it was $(H_{chi} + \frac{H_{col}}{2})$ as given by Eq. (23). They are $G_s = 1000$ W/m^2, $A_{col} = 950 \times 10^3$ m^2 (equivalent to $D_{col} = 1100$ m), $T_0 = 293$ K. For a triangular collector field with identical base and height as in Fig. 1(b), the collector height, H_{col} is calculated from the collector layout as

$$H_{col} = (2 \times A_{col})^{\frac{1}{2}} \times \sin\beta_{opt} \tag{29}$$

Actually, to accommodate the turbine and chimney, the collector field has a trapezoidal shape with its apex quite small compared to its base, hence it is approximated here with a triangle.

To calculate collector height, with optimum slope at each location, i.e. $\beta = 38.4°$ for Ottawa, 45.1° for Winnipeg and 48.4° for Edmonton and using Eq. (29), the collector height, H_{col} is determined. They are 848, 975 and 1024 m respectively. Since the highest elevation is for Edmonton, in order to install a vertical axis turbine of 54 m nominal diameter in a diffuser like cylindrical pipe, a chimney of 35 m high is selected. The total equivalent chimney height is then $H_{col}/2 + H_{chi} \approx 547$ m. For the same equivalent chimney height, the chimney height for the other locations is 123 m for Ottawa and 60 m for Winnipeg. The nominal power is calculated as 4.97 MW for each case, including that of reference for which the same equivalent chimney height is used. The height of the collector cover from the ground is about 1.7 m at the air entrance at the base of the collector field and is gradually increased to about 10 m at the top. The preliminary design data are summarized in Table 2.

We note that the preliminary design parameters in Table 2 are selected and determined for a nominal solar intensity of 1000 W/m^2 and consequently they are for a nominal plant power of 5 MW. In reality, the plant power is calculated based on the simulation for whole year and using the monthly average radiation data, with a maximum intensity lower than 1000 W/m^2. Thus, the calculated power as well as other parameters are dy-

Table 2
Preliminary design parameters for 5 MW solar chimney power plant

	Ottawa	Winnipeg	Edmonton	Schlaich (1995)
Collector diameter (m)	–	–	–	1110
Collector area (m^2)	950 000	950 000	950 000	950 000
Chimney height (m)	123	60	35	547
Collector height (m)	848	975	1024	–
Chimney diameter (m)	54	54	54	54
Temperature rise in collector (°C)	25.9	25.9	25.9	25.9
Updraught velocity (m/s)	9.1	9.1	9.1	9.1
Total pressure head (Pa)	518.3	518.3	518.3	383.3
Average efficiency				
Collector (%)	56.00	56.00	56.00	56.24
Chimney (%)	1.82	1.82	1.82	1.45
Turbine (%)	77.0	77.0	77.0	77.0
Whole system (%)	0.79	0.79	0.79	0.63

Table 1
Optimum slope and calculated parameters

Location	ϕ (°)	β_{opt} (°)	$\Sigma\bar{H}$ (kW h/m^2/year)	$\Sigma\bar{H}_T$ (kW h/m^2/year)	$\Sigma\bar{S}$ (kW h/m^2/year)	$\Sigma\bar{q}_u$ (kW h/m^2/year)
Ottawa	45.5	38.4	1327	1545	1191	697
Winnipeg	49.9	45.1	1365	1712	1327	796
Edmonton	53.6	48.4	1299	1697	1318	793

namic and vary throughout the year. In our case, 12 monthly average values are calculated by the code.

Monthly average solar radiation on the horizontal surface $\bar{H}$, on the collector surface $\bar{H}_T$, on absorber or ground, $\bar{S}$ and the useful collected energy, $\bar{Q}_u$ all in MJ/m^2/day are shown in Fig. 3 for Winnipeg. The annual values are shown also in the inset. We can see that the global radiation on the horizontal surface follows the usual trend with a maximum during June and July, and unfavorable global radiation during November–January. $\Sigma\bar{H} = 4914$ MJ/m^2/year or 1365 kW/m^2/year may not be considered very favorable for chimney power plants with horizontal collector layout. With the optimum slope for collector layout, the monthly average global solar radiation on the collector, $\bar{H}_T$ has a better distribution through the year and $\Sigma\bar{H}_T$ =6163 MJ/m^2/year or 1712 kW h/m^2/year is increased by about 25% with respect to that on the horizontal surface. As expected, the solar energy $\bar{S}$ on the ground under the collector roof and the useful energy $\bar{Q}_u$ follow the variation of $\bar{H}_T$. The difference $\bar{H}_T - \bar{S}$ is the collector optical transmission loss and $\bar{S} - \bar{Q}_u$ is the collector heat transfer losses. Similar results were obtained with the other two locations, the annual results of which are presented in Table 1.

To obtain thermal performance at the three locations, the simulation is done using the preliminary design parameters. The results are presented in Figs. 4–6. Power in MW and monthly electric energy production in GW h/month as a function of month for three locations are presented in Fig. 4. The variation of power is a little different from that of the monthly average of the useful energy collected of Fig. 3. The reason is due to the simulation method used: the power is proportional to the monthly average collected energy per day divided by the duration of a typical day. The duration is short during winter months and long during summer months, thus the same order of energy is produced by a smaller turbine power during summer months. For Winnipeg for example, the duration is about 6–9 h in winter months and 13–15 h during summer months, yet the useful energy collected in Fig. 3 is about the same at 8–9 MJ/m^2/day. As we will see later, for smaller slopes than the optimum, the situation will be different. The lower group of curves in Fig. 4 shows the electric energy produced. It seems the electric energy production is almost the same for the three locations and their variation through the year is less pronounced, which is expected following our observation regarding power. The annual electric energy production is 6.78 GW h/year for Ottawa, 7.78 for Winnipeg and 7.81 for Edmonton.

For a comparison with southern locations where horizontal collector system can be installed, we chose El Paso TX with $\phi = 31.80°$, $\Sigma\bar{H} = 2185$ kW h/m^2/year, and simulated the same chimney plant as in Table 2.

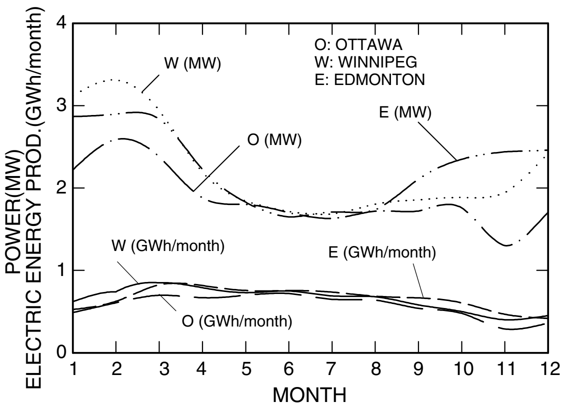

Fig. 4. Power and electric energy production as a function of month for the three locations. Locations are shown with their first letter followed by power as MW in parentheses and energy as GW h/month in parentheses.

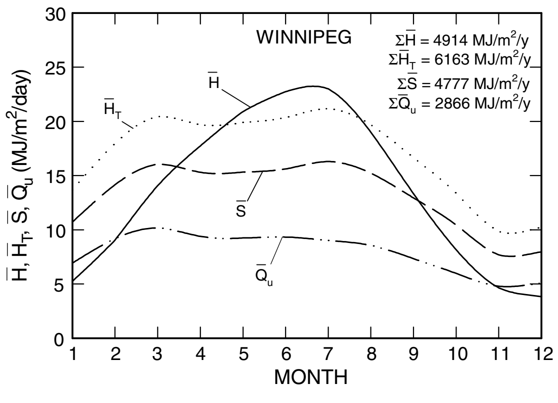

Fig. 3. Monthly average daily solar radiation on horizontal, on collector surface, on the absorber ground and useful collected energy as a function of month for Winnipeg.

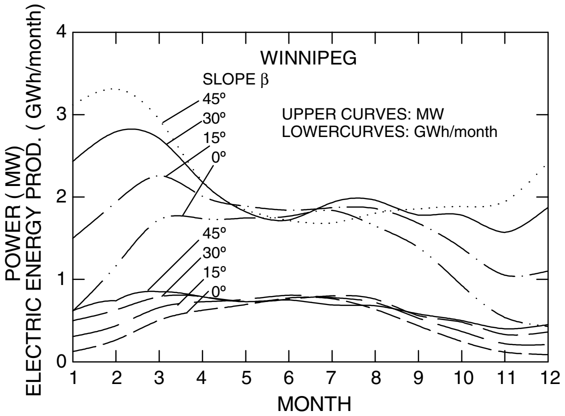

Fig. 5. Power and electric energy production as a function of month with collector slope as a parameter for Winnipeg.

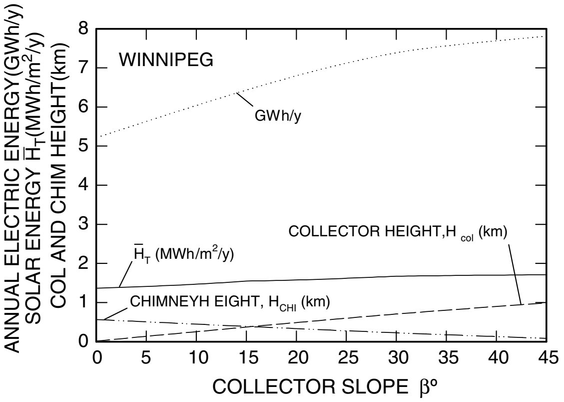

Fig. 6. Annual electric energy production, monthly average daily solar energy on the collector, collector and chimney heights as a function of collector slope for Winnipeg.

The annual electric energy production was 9.13 GW h/year, which is about 15% higher than the best case in northern latitudes considered in this study. We see that solar chimney plants in higher latitudes may be feasible if the cost reduction of the chimney versus the possible cost increase in sloped collector system is more pronounced. Indeed, according to Schlaich (1995), the costs for the collector system, chimney and mechanical system are 40%, 31% and 17% of the total cost respectively, in small plants of 5 MW size. Thus, even if the part of the cost reduction in chimney system is spent for the increased cost of sloped collector system, it may result in economically feasible electric energy cost. This aspect must however be studied by costing in detail alternative designs for specific site and plant size.

The effect of the collector slope on power and electric energy production as a function of month with slope as a parameter is presented in Fig. 5 for Winnipeg. Following our observation regarding Fig. 4, we see that as the slope is smaller than the optimum, power variation through the year becomes less affected by the duration of typical days. In fact, for $\beta = 0$, the power variation follows that of $\bar{H}$ in Fig. 3. The monthly electric energy production in lower group of curves shows that the energy production is reduced when the slope is decreased. The annual electric energy production with various slopes is: 5.21 GW h/year for $\beta = 0°$, 6.42 for 15°, 7.37 for 30° and 7.78 for 45°. This shows that maximizing the solar energy on the collector system may not be absolutely necessary, and depending on availability of mountain hills, even with variable slopes, a solar chimney power plant can be designed and built if the economic feasibility requirements are satisfied.

To see the sensitivity of various parameters on the slope from 0° to 45°, a study was carried out for the case of Winnipeg. The results are presented in Fig. 6. The collector height varies almost linearly from zero at $\beta = 0°$ to 975 m at $\beta = 45°$, the chimney height varies also similarly from 547 m to 60 m. The solar radiation on the collector surface varies non-linearly from 4.97 GJ/m^2/year at $\beta = 0°$ to 6.16 GJ/m^2/year $\beta = 45°$. The electric energy production varies non-linearly from 5.21 GW h/year for $\beta = 0°$ to 7.78 for 45° as noted earlier. We see that between $\beta = 20°$ and 45°, the electric energy production is affected only by about 13%, which means the hills with slope range from 20° to 45° can be easily used in combination of variable sloped collectors. In general, if hills with variable slope are identified, they may be considered for further study and simulation, since based on the results of Fig. 6, the annual electric energy production may not be penalized as much and the economic feasibility requirements may be satisfied easier.

The overall thermal efficiency of the solar chimney power plant at three locations is $\eta = 0.458\%$ for Ottawa, 0.478% for Winnipeg and 0.484% for Edmonton. In comparison, the thermal efficiency of the El Paso plant is $\eta = 0.436\%$. The reason for better performance of the plants at high latitudes, the temperature rise in the collector is only from 5 to 10 K as a result of which the collector efficiency is higher by about 2% than that at El Paso with horizontal collector field where the temperature rise is almost twice as much.

5. Conclusions

We presented in this study solar chimney power plants at high latitudes. To evaluate them, we developed a mathematical model and a code on MATLAB platform based on monthly average meteorological data and a thermodynamic cycle. The thermal performance of a 5 MW nominal power production plant at three locations in Canada, namely Ottawa, Winnipeg and Edmonton, is studied. The sloped collector field is built at suitable mountain hills, which also functions as a chimney. Then a short vertical chimney is added to install the vertical axis air turbine.

The results showed that

- Despite less favorable solar radiation on horizontal planes in higher latitudes the annual electric energy production may be as high as 85% of that which would be produced in best favorable locations from the same plants with horizontal collector field.
- For a typical location, the chimney height may be reduced by almost 90%, which may result in considerable saving of initial investment as well as in elimination of civil engineering problems, which are also related to operation and maintenance cost. Although this is true, the cost of collector field on hills may be increased due to civil work on sloped surfaces. This aspect should be studied in detail for site specific cases.

- Since natural hills will be used for collector field the slope may be variable. It is predicted that the overall performance will not be penalized more than 13%, if the slope varies by 20–25° from the optimum slope.
- The overall thermal performance of the solar chimney power plants at high latitudes is about 0.48%, which is slightly better than that with horizontal collector fields at southern locations with favorable climate.

Acknowledgement

The financial support for this project by Natural Sciences and Engineering Research Council of Canada is acknowledged.

References

Azevedo, L.F.A., Sparrow, E.M., 1985. Natural convection in open-ended inclined channels. J. Heat Transfer 107, 893–901.

Bernardes, M.A., Dos, S., Voss, A., Weinrebe, G., 2003. Thermal and technical analyses of solar chimneys. Solar Energy 75, 511–524.

Churchill, S.W., Chu, H.H.S., 1975. Correlating equations for laminar and turbulent free convection from a vertical plate. Int. J. Heat Mass Transfer 18, 1323–1329.

Duffie, J.A., Beckman, W.A., 1991. Solar Engineering of Thermal Processes. Wiley Interscience, New York.

Enviromission, 2004. Available from: <www.enviromission.com.au>.

Fujii, T., Imura, H., 1972. Natural convection from a plate with arbitrary inclination. Int. J. Heat Mass Transfer 15, 755–767.

Haaf, W., 1984. Part II: Preliminary test results from the Manzanares pilot plant. Int. J. Solar Energy 2, 141–161.

Haaf, W., Friedrich, G., Mayr, G., Schlaich, J., 1983. Part I: Principle and construction of the pilot plant in Manzanares. Int. J. Solar Energy 2, 3–20.

Ingersoll, L.R., Zobel, O.J., Ingersoll, A.C., 1954. Heat Conduction (with Engineering, Geological and Other Applications). The University of Wisconsin Press, New York.

Klein, S.A., 1979. Calculation of the monthly average transmittance–absorptance product. Solar Energy 23, 547–551.

McAdams, W.H., 1954. Heat Transmission, third ed. McGraw-Hill, New York.

Pasumarthi, N., Sherif, S.A., 1998. Experimental and theoretical performance of a demonstration solar chimney model—Part I: mathematical model development. Int. J. Energy Research 22, 277–288.

Schlaich, J., 1995. The Solar Chimney: Electricity from the Sun. Axel Menges, Stuttgart.